Title

Brain putamen volume changes in newly-diagnosed patients with obstructive sleep apnea

Authors

Kumar, Rajesh
Farahvar, Salar
Ogren, Jennifer A
et al.

Publication Date

2014

DOI

10.1016/j.nicl.2014.01.009

NeuroImage: Clinical 4 (2014) 383–391

Contents lists available at ScienceDirect

NeuroImage: Clinical

journal homepage: www.elsevier.com/locate/ynicl

Brain putamen volume changes in newly-diagnosed patients with obstructive sleep apnea

Rajesh Kumar [a,b,e,*], Salar Farahvar [c], Jennifer A. Ogren [d], Paul M. Macey [d,e], Paul M. Thompson [f,g], Mary A. Woo [d], Frisca L. Yan-Go [f], Ronald M. Harper [c,e]

[a] Department of Anesthesiology, David Geffen School of Medicine at UCLA, University of California at Los Angeles, Los Angeles, CA 90095, USA
[b] Department of Radiological Sciences, David Geffen School of Medicine at UCLA, University of California at Los Angeles, Los Angeles, CA 90095, USA
[c] Department of Neurobiology, David Geffen School of Medicine at UCLA, University of California at Los Angeles, Los Angeles, CA 90095, USA
[d] UCLA School of Nursing, University of California at Los Angeles, Los Angeles, CA 90095, USA
[e] The Brain Research Institute, University of California at Los Angeles, Los Angeles, CA 90095, USA
[f] Department of Neurology, David Geffen School of Medicine at UCLA, University of California at Los Angeles, Los Angeles, CA 90095, USA
[g] Department of Psychiatry, David Geffen School of Medicine at UCLA, University of California at Los Angeles, Los Angeles, CA 90095, USA

ARTICLE INFO

Article history:
Received 2 August 2013
Received in revised form 17 January 2014
Accepted 21 January 2014
Available online 31 January 2014

Keywords:
Magnetic resonance imaging
Cognition
3D surface morphometry
Basal ganglia
Intermittent hypoxia
Autonomic
Motor

ABSTRACT

Obstructive sleep apnea (OSA) is accompanied by cognitive, motor, autonomic, learning, and affective abnormalities. The putamen serves several of these functions, especially motor and autonomic behaviors, but whether global and specific sub-regions of that structure are damaged is unclear. We assessed global and regional putamen volumes in 43 recently-diagnosed, treatment-naïve OSA (age, 46.4 ± 8.8 years; 31 male) and 61 control subjects (47.6 ± 8.8 years; 39 male) using high-resolution T1-weighted images collected with a 3.0-Tesla MRI scanner. Global putamen volumes were calculated, and group differences evaluated with independent samples t-tests, as well as with analysis of covariance (covariates; age, gender, and total intracranial volume). Regional differences between groups were visualized with 3D surface morphometry-based group ratio maps. OSA subjects showed significantly higher global putamen volumes, relative to controls. Regional analyses showed putamen areas with increased and decreased tissue volumes in OSA relative to control subjects, including increases in caudal, mid-dorsal, mid-ventral portions, and ventral regions, while areas with decreased volumes appeared in rostral, mid-dorsal, medial-caudal, and mid-ventral sites. Global putamen volumes were significantly higher in the OSA subjects, but local sites showed both higher and lower volumes. The appearance of localized volume alterations points to differential hypoxic or perfusion action on glia and other tissues within the structure, and may reflect a stage in progression of injury in these newly-diagnosed patients toward the overall volume loss found in patients with chronic OSA. The regional changes may underlie some of the specific deficits in motor, autonomic, and neuropsychologic functions in OSA.

1. Introduction

Obstructive sleep apnea (OSA) patients show multiple neurobehavioral difficulties, including deficits in attention, psychomotor and executive functioning, memory, and affect (Beebe et al., 2003). However, the principal deficits in the syndrome involve the loss of motor control over the upper airway muscles, which fail to discharge in a timely fashion, when they should dilate the airway during diaphragmatic descent, and a loss of control over autonomic motor activity, with chronic, exaggerated sympathetic discharge (Somers et al., 1995), and inappropriate lagged or muted dynamic sympathetic responses to blood pressure or ventilatory challenges (Harper et al., 2003; Henderson et al., 2004; Macey et al., 2006). Those somatic and autonomic motor defects suggest central injury in motor and autonomic regulatory structures, and gross damage has been found in multiple sites, based on manual and voxel-based morphometry of high-resolution T1-weighted images (Kumar

Abbreviations: OSA, Obstructive sleep apnea; 3D, Three dimensional; MRI, Magnetic resonance imaging; AHI, Apnea–hypopnea index; ESS, Epworth Sleepiness Scale; PSQI, Pittsburgh Sleep Quality Index; BDI-II, Beck Depression Inventory II; BAI, Beck Anxiety Inventory; PD, Proton density; MNI, Montreal Neurological Institute; CSF, Cerebrospinal fluid; TIV, Total intracranial volume; MPRAGE, Magnetization prepared rapid acquisition gradient-echo; TR, Repetition time; TE, Echo time; FA, Flip angle; FOV, Field of view; GRAPPA, Generalized autocalibrating partially parallel acquisition.

* Corresponding author at: Department of Anesthesiology, David Geffen School of Medicine at UCLA, 56-132 CHS, 10833 Le Conte Av, University of California at Los Angeles, Los Angeles, CA 90095-1763, USA. Tel.: +1 310 206 1679, +1 310 206 6133; fax: +1 310 825 2224.
E-mail address: rkumar@mednet.ucla.edu (R. Kumar).

http://dx.doi.org/10.1016/j.nicl.2014.01.009

et al., 2008; Macey et al., 2002), diffusion tensor imaging (Kumar et al., 2012; Macey et al., 2008), and T2-relaxometry procedures (Cross et al., 2008; Kumar et al., 2009b). Several of the affected brain sites include structures that serve both somato motor and autonomic motor roles; one such structure is the putamen, which shows overall injury, metabolic abnormalities, and functional deficits (Alkan et al., 2013; Emin Akkoyunlu et al., 2013; Kumar et al., 2012; Macey et al., 2006).

The evidence for putamen roles in autonomic regulation is well-known, especially from pathological conditions with dysautonomia, such as Multiple Systems Atrophy (Pastakia et al., 1986). Such a role is expected, considering the major projections received from the autonomic regulatory insular cortices (Saper, 1982). The putamen somatic motor role appears to incorporate sensory and other signals to initiate effective motor action, with putamen stroke inducing conditions of "motor neglect" (Sapir et al., 2007). OSA represents a prime example of how signals fail to initiate and maintain upper airway muscle discharge, and the putamen may be playing a significant role in that upper airway muscle "neglect," particularly considering its projections to brain areas regulating oral motor functions (Kunzle, 1978; Miyata and Sasaki, 1984).

The putamen also contributes to regulation of other neuropsychologic, cognitive, and learning functions which are deficient in OSA. These functions include memory, mood, language, and motivation, show differential topographic organization (Alexander and Crutcher, 1990; Badgaiyan et al., 2008; Booth et al., 2007; Bowman et al., 1996; Husain et al., 1991; Saper, 1982), and the sub-regions within that organization receive information from prefrontal, insular, and thalamic areas, and send dopaminergic projections to the ventral tegmentum, substantia nigra, and globus pallidus (Avendano et al., 2006; DeVito et al., 1980; Ferry et al., 2000; Gorbachevskaya, 1997; Saper, 1982; Schultz and Romo, 1987). Putamen volumes are reduced in depressed patients (Husain et al., 1991), and over half of OSA patients are depressed (Asghari et al., 2012); the majority of OSA subjects also show learning deficits (Wallace and Bucks, 2013).

Regional structural changes within the putamen can thus alter information transfer between various brain sites. Manual volumetric procedures, using high-resolution T1-weighted images, can evaluate global putamen volume (Kumar et al., 2011), and 3D surface morphometry techniques can assess regional tissue changes, as well as extent of changes within the structures (Butters et al., 2009; Sabattoli et al., 2008; Shi et al., 2013; Thompson et al., 2004). Both procedures have been used to examine global and regional basal ganglia structures (Kumar et al., 2009a), including the putamen (Kumar et al., 2011). The extent of tissue changes within putamen sub-regions which serve specialized functions, or project to other brain areas serving unique roles, is unclear in OSA. Knowledge of localized changes is essential to disclose functional outcomes, since the functional topography of the putamen is not uniform.

Our aim was to examine global and regional putamen volumes in OSA relative to control subjects using high-resolution T1-weighted images with manual volumetric and 3D surface morphometry procedures, and to determine the nature of any volume changes. We selected newly-diagnosed, untreated OSA patients to avoid confounding measures with treatment interventions, and to determine tissue changes as early as possible in the syndrome development. Since OSA subjects show overall putamen damage, altered metabolites, and functional deficits (Alkan et al., 2013; Emin Akkoyunlu et al., 2013; Kumar et al., 2012; Macey et al., 2006) and severe autonomic, behavioral and motor deficits appear in the condition, we hypothesized that both left and right global and regional putamen integrity would be altered in OSA, compared to control subjects.

2. Materials and methods

2.1. Subjects

We studied 43 recently-diagnosed (based on overnight polysomnography; apnea–hypopnea-index ≥ 5) OSA subjects before any treatment, and 61 healthy control subjects. Both OSA and control subjects included here were subjects in previously-published manuscripts related to other issues in OSA (Cross et al., 2008; Kumar et al., 2008, 2009b, 2012; Macey et al., 2008, 2010, 2012, 2013). All OSA subjects were recruited from the Sleep Disorders Laboratory at UCLA, and control subjects were recruited from the UCLA campus and West Los Angeles area. OSA subjects were not taking any medications (β-blockers, α-agonists, angiotension-converting enzyme inhibitors, vasodilators, or serotonin reuptake inhibitors), and were without any diagnosed history of stroke, heart failure, or mental illness that might influence brain tissue composition. Control subjects were in good health, without any brain disorder which may induce brain tissue changes. We interviewed the control subjects, as well as their sleep partners, when available, to determine the potential for sleep disordered breathing, and subjects suspected of having such disturbed patterns underwent an overnight sleep study. OSA and control subjects with body weight more than 125 kg (scanner limitation), or with MRI incompatible metallic implants were excluded, as described at the MRI safety website (http://www.mrisafety.com/). All OSA and control subjects gave written and informed consent prior to the study, and the study protocol was approved by the Institutional Review Board at the University of California at Los Angeles.

2.2. Overnight polysomnography (PSG)

Overnight sleep studies were performed on all OSA subjects at the UCLA Sleep Disorders Center and Laboratory, and consisted of a 7–10 hour period (9:00 PM to 6:00 AM) monitoring of electroencephalogram (EEG — central and occipital), digastric electromyogram (EMG), electrocardiogram (EKG — lead II), right and left extra-ocular eye movement (EOG), thoracic and abdominal wall movement, air flow, O_2 saturation, end-tidal CO_2 levels, snore volume, bilateral leg movement, and sleep position. Acquired data were digitized, and stored on a computer for sleep evaluation.

2.3. Examination of daytime sleepiness and sleep quality

We used the Epworth Sleepiness Scale (ESS) and the Pittsburgh Sleep Quality Index (PSQI) questionnaires to examine daytime sleepiness and sleep quality, respectively, in both OSA and control subjects (Johns, 1991; Knutson et al., 2006). These commonly-used measures were self-administered, either before or after MRI data acquisition.

2.4. Assessment of depression and anxiety symptoms

We administered the Beck Depression Inventory (BDI)-II to examine depressive symptoms, and the Beck Anxiety Inventory to assess anxiety symptoms in OSA and control subjects (Beck et al., 1988, 1996), either before or after MRI data collection. Both inventories are self-administered questionnaires, with scores between 0 and 63, based on the severity of symptoms (Beck et al., 1988, 1996).

2.5. Magnetic resonance imaging

Brain studies were performed using a 3.0-Tesla MRI scanner (Magnetom Tim-Trio; Siemens, Erlangen, Germany), with a receive-only 8-channel phased-array head-coil, and a whole-body transmitter coil. Foam pads were used on both sides of the head to reduce head motion related artifacts, and subjects lay supine during data collection. We collected two high-resolution T1-weighted image scans using a magnetization prepared rapid acquisition gradient-echo (MPRAGE) pulse sequence [repetition time (TR) = 2200 ms; echo time (TE) = 2.2 ms; inversion time = 900 ms; flip angle (FA) = 9°; matrix size = 256 × 256; field of view (FOV) = 230 × 230 mm; slice thickness = 1.0 mm; slices = 176]. Proton density (PD) and T2-weighted images were collected using a dual-echo turbo spin-echo pulse sequence (TR = 10,000 ms; TE1,

2 = 17, 134 ms; FA = 130°; matrix size = 256 × 256; FOV = 230 × 230 mm; slice thickness = 4.0 mm; slices = 55; turbo factor = 5). Diffusion tensor imaging data were acquired using a single-shot echo-planar imaging with twice-refocused spin-echo pulse sequence (TR = 10,000 ms; TE = 87 ms; flip angle = 90°; band-width = 1346 Hz/pixel; matrix size = 128 × 128; FOV = 230 × 230 mm; slice thickness = 2.0 mm, b = 0 and 700 s/mm^2, diffusion directions = 12). Four separate DTI series were collected with the same imaging protocol for subsequent averaging. We used a parallel imaging technique, "generalized autocalibrating partially parallel acquisition (GRAPPA)", with an acceleration factor of two for all scans.

2.6. Data processing and analysis

2.6.1. Overnight PSG data

All sleep recordings were interpreted by the UCLA sleep physicians. Sleep states, sleep disordered breathing, and physiology were assessed first for total sleep time, and number and type (central, obstructive, or mixed — based on air flow and thoracic and abdominal strain gauges) of apneic episodes. Sleep records were scored by a registered PSG technician, and then each PSG was reviewed by the sleep physician. Using the digitized PSG signals, each one-min data epoch were scored as awake (W), rapid-eye movement sleep (R), or sleep stages N1–N3, based on recently-revised scoring criteria (Iber et al., 2007). The apnea–hypopnea-index (AHI), is a severity index of sleep disordered breathing, combining both apneas and hypopneas, and is calculated by dividing the number of apnea and hypopnea by the total sleep time. Subjects were classified as having OSA based on an AHI ≥ 5/h (1999). OSA was classified as "moderate" if AHI > 15, and "severe" if AHI > 30 (1999). The total number and duration of apnea, AHI, number of arousals, O_2 saturation variables, total sleep time, time in each state, and sleep efficiency variables were calculated.

2.6.2. MRI data

High-resolution T1-weighted, PD-, and T2-weighted scans were visually-examined to assess any major brain lesions (e.g., cystic lesions, major infarcts, or space occupying lesions). Both high-resolution T1-weighted scans were also examined for any imaging artifacts before data processing.

We used the statistical parametric mapping package SPM8 (http://www.fil.ion.ucl.ac.uk/spm/), MRIcroN, and MATLAB-based (The MathWorks Inc., Natick, MA) custom software for data processing, manually-outlining putamen structures, and determination of putamen volumes.

2.6.2.1. Realignment, averaging, and rigid-body transformation. We realigned both high-resolution T1-weighted scans to remove any potential variations between the two series, and averaged the images using SPM8 software. Averaged images of individual subjects, using unified segmentation, were bias-corrected for regional signal intensity differences, and image volumes were reoriented into Montreal Neurological Institute (MNI) common space with an affine transformation (Kumar et al., 2011). The affine-transformed images were resampled to a voxel size of 0.9 × 0.9 × 0.9 mm, and used to outline manually putamen structures (Kumar et al., 2011).

2.6.2.2. Gray matter, white matter, and cerebrospinal fluid and intracranial volume calculation. The averaged and reoriented images of individual subjects were partitioned into gray, white, and cerebrospinal fluid (CSF) probability maps using the unified segmentation method. Within the gray, white, and CSF probability maps, all voxels with a probability value >0.5 were counted, and whole-brain gray, white, and CSF volumes were calculated. Whole-brain gray, white, and CSF volumes were added to determine total intracranial volume (TIV).

2.6.2.3. Putamen tracing and global volume quantification. We used the reoriented and resampled brain scans to manually-outline both left and right putamen structures with MRIcroN software. One investigator, who was blinded for subject group assignments, outlined putamen structures in all OSA and control subjects, based on a protocol described earlier (Kumar et al., 2011). Using these tracings, left and right global putamen volumes were calculated (Kumar et al., 2011).

2.6.2.4. Calculation of putamen mean diffusivity (MD) values. DTI data were processed as described previously (Kumar et al., 2012). Briefly, using diffusion weighted and non-diffusion weighted images, diffusion tensor matrices were calculated, matrices diagonalized, and principal eigenvalues were calculated. The principal eigenvalues were used to calculate MD maps, as described earlier (Kumar et al., 2012).

MD maps, derived from each DTI series, were realigned, averaged to create one MD map per subject, and averaged MD maps were normalized to a common space. Similarly, non-diffusion images were realigned, averaged, and normalized to a common space. All normalized non-diffusion images were averaged to determine a background image, which was used to create left and right putamen regions-of-interest masks, guided by the previous findings (Kumar et al., 2012). Using the normalized MD maps and left and right putamen region-of-interest masks, average left and right MD values were derived.

2.6.2.5. Intra-tracer reliability. We examined intra-tracer reliability for outlining putamen structures by re-outlining those structures in 10 randomly-selected OSA and 10 control subjects by the same investigator who outlined structures in all OSA and control subjects. Total putamen volumes were used for intra-tracer reliability calculations. Intra-tracer reliability was high for putamen tracings (intra-class correlation = 0.91, $p < 0.001$), indicating consistent tracings across all subjects.

2.6.2.6. 3D Surface morphometry. We used 3D surface morphometry to visualize regional putamen volume variations between OSA and control subjects (Butters et al., 2009; Sabattoli et al., 2008; Shi et al., 2013; Thompson et al., 2004). Both left and right surface models were created from individual putamen tracings, and 3D meshes were generated in which each mesh consisted of a fixed number of equally-spaced points. A medial curve representing center of mass was determined in the anterior–posterior direction within each mesh, and using the medial curve, the thickness of the putamen (radial distance) was calculated at each surface point (Thompson et al., 2004). To visualize the local volume of putamen sub-regions in the OSA, relative to the control group, the ratio of mean radial distances at each surface point (OSA/control) was calculated, color-coded (*orange to red*, volume losses; *blue to purple*, volume increases), and overlaid onto averaged 3D putamen surface models, determined by averaging all OSA and control surface models.

2.7. Statistical analysis

Data were evaluated using the IBM Statistical Package for the Social Sciences (IBM SPSS, V 20). We examined numerical demographic, biophysical, sleep, and neuropsychologic data (age, body mass index, ESS, PSQI, BDI-II, and BAI) with independent samples t-tests, and categorical demographic data (gender) with Chi-square tests. Global putamen volumes, putamen MD values, gray matter, white matter, CSF, and TIV values were examined between groups using independent samples t-tests. Global putamen volumes and putamen MD values were also examined with analysis of covariance, with age, gender, and TIV included as covariates for putamen volumes, and age and gender as covariates for MD values. Pearson's correlation procedures were used to examine the association between global putamen volumes and BMI, sleep variables, neuropsychologic scores, putamen MD values, and O_2 saturation variables in OSA subjects. We used linear regression analysis to determine the impact of clinical, biophysical, and O_2 saturation values on global putamen volumes of OSA subjects. The dependent variables were left

and right putamen volumes, and independent variables were AHI, BMI, ESS, PSQI, BDI-II, BAI, and O_2 saturation nadir values. We established intra-tracer reliability with an intra-class correlation procedure.

3. Results

3.1. Demographics

Demographic data are summarized in Table 1. Neither age nor gender differed significantly between OSA and control subjects (age, $p = 0.56$; gender, $p = 0.38$). Body mass indices were significantly higher in OSA compared to control subjects ($p < 0.001$).

3.2. Sleep, O_2 saturation, and neuropsychologic variables

Sleep, O_2 saturation, and neuropsychologic variables of OSA and control subjects are summarized in Table 1. Both ESS and PSQI scores significantly differed between OSA and control subjects (ESS, $p < 0.001$; PSQI, $p < 0.001$). BDI-II and BAI values were significantly higher in OSA, compared to control subjects (BDI-II, $p < 0.001$; BAI, $p = 0.001$).

3.3. Global gray, white, and CSF volumes and TIV

Global gray matter, white matter, CSF volumes, and TIV values of OSA and control group are summarized in Table 1. Gray matter, white matter, and CSF volumes, as well as TIV values, did not differ significantly between OSA and control subjects (gray matter, $p = 0.40$; white matter, $p = 0.27$; CSF, $p = 0.62$; TIV, $p = 0.82$).

3.4. Global putamen volumes and MD value differences

Both left and right global putamen volumes of OSA and control subjects are summarized in Table 1, and scatter plots are shown in Fig. 1. The left and right global putamen volumes were significantly higher in OSA, compared to control subjects (independent samples t-tests; left, $p = 0.041$; right, $p = 0.025$); values were significantly higher in OSA, even after controlling for age, gender, and TIV (ANCOVA; left, $p = 0.043$; right, $p = 0.027$).

Average putamen MD values of OSA and control subjects are summarized in Table 1. Both left and right putamen MD values were significantly lower in OSA, compared to control subjects (independent samples t-tests; left, $p = 0.017$; right, $p = 0.001$); values were

Table 1
Characteristics of OSA and control subjects.

Variable type	Variables	OSA (Mean ± SD) [A]	Controls (Mean ± SD) [B]	[A] vs [B] *p* values
Demographic	Age (years)	46.4 ± 8.8 (n = 43)	47.4 ± 8.9 (n = 61)	0.56
	Gender (Male:Female)	31:12	39:22	0.38
Biophysical	BMI (kg/m^2)	30.1 ± 5.2 (n = 43)	24.8 ± 3.7 (n = 61)	< 0.001*
Sleep	AHI (events/h)	31.4 ± 19.3 (n = 43)	–	–
	ESS	10.3 ± 4.9 (n = 43)	5.5 ± 3.5 (n = 61)	< 0.001*
	PSQI	9.3 ± 4.0 (n = 43)	3.8 ± 2.5 (n = 61)	< 0.001*
O_2 saturation	Baseline SaO_2 (%)	96.3 ± 2 (n = 40)	–	–
	SaO_2 nadir (%)	77.9 ± 10.3 (n = 36)	–	–
	SaO_2 nadir change (%)	18.3 ± 10.6 (n = 36)	–	–
	Obstructive length of nadir (s)	40.6 ± 21.4 (n = 30)	–	–
Neuropsychological	BDI-II	9.3 ± 8.3 (n = 43)	3.9 ± 4.4 (n = 61)	<0.001*
	BAI	10.7 ± 12.4 (n = 43)	3.9 ± 5.0 (n = 61)	0.001*
Brain (volume)	Gray matter (mm^3)	700,469.7 ± 73,557.7 (n = 43)	713,303.3 ± 77,941.7 (n = 61)	0.40
	White matter (mm^3)	445,347.5 ± 56,252.4 (n = 43)	458,578.8 ± 63,000.5 (n = 61)	0.27
	CSF (mm^3)	315,275.5 ± 167,583.0 (n = 43)	298,249.2 ± 175,544.6 (n = 61)	0.62
	TIV (mm^3)	1,461,092.6 ± 206,276.6 (n = 43)	1,470,131.3 ± 199,550.1 (n = 61)	0.82
Putamen (volume)	Left putamen (mm^3)	4146.6 ± 666.0 4117.9 ± 461.6 (n = 43)	3909.1 ± 502.4 3929.3 ± 461.1 (n = 61)	0.041 0.043**
	Right putamen (mm^3)	4152.8 ± 654.5 4125.2 ± 465.2 (n = 43)	3897.6 ± 487.8 3917.0 ± 472.3 (n = 61)	0.025 0.027**
Putamen (MD values)	Left putamen ($\times 10^{-6}$ mm^2/s)	803.17 ± 75.64 802.58 ± 84.52 n = 19	870.00 ± 92.30 870.50 ± 84.48 n = 21	0.017 0.016##
	Right putamen ($\times 10^{-6}$ mm^2/s)	784.75 ± 67.94 784.23 ± 91.68 n = 19	889.12 ± 112.18 889.58 ± 91.65 n = 21	0.001 0.001##

SD, standard deviation; BMI, body mass index; AHI, apnea–hypopnea-index; ESS, Epworth Sleepiness Scale; PSQI, Pittsburgh Sleep Quality Index; SaO_2, O_2 saturation; BDI-II, Beck Depression Inventory II; BAI, Beck Anxiety Inventory; CSF, cerebrospinal fluid; TIV, total intracranial volume; *, equal variances not assumed; **, p value adjusted for age, gender, and TIV; ##, p value controlled for age and gender.

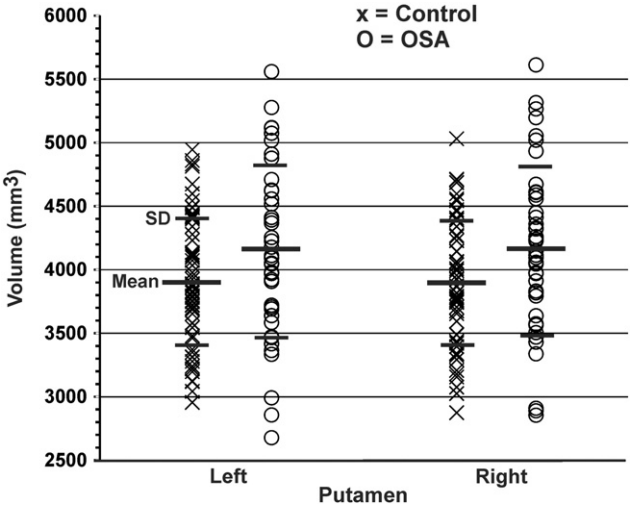

Fig. 1. Global putamen volumes of OSA and control subjects. Both left and right putamen volumes were significantly increased in recently-diagnosed, treatment naïve OSA over control subjects, controlling for age, gender, and TIV (left, $p = 0.043$; right, $p = 0.027$).

significantly reduced in OSA over controls, even accounting for age and gender (ANCOVA; left, $p = 0.016$; right, $p = 0.001$).

3.5. Relationships between global putamen volumes and BMI, sleep, O_2 saturation, left and right putamen md values, and neuropsychologic variables

Coefficients of correlation and significance levels among putamen volumes, BMI, sleep, O_2 saturation, left and right putamen MD values, and neuropsychologic variables are tabulated in Table 2. Significant negative correlations appeared between global putamen volumes, BMI (left; $r = -0.35$ $p = 0.022$; right, $r = -0.32$, $p = 0.036$), and putamen MD values (left; $r = -0.48$, $p = 0.035$; right, $r = -0.46$, $p = 0.047$) in OSA subjects. However, no significant correlations emerged between putamen volumes and AHI, PSQI, or ESS scores. The BAI scores significantly correlated with putamen volumes (left; $r = -0.39$ $p = 0.01$; right, $r = -0.40$, $p = 0.008$); however, BDI-II scores did not show any correlations. The O_2 desaturation nadir showed a significant association with left putamen volume ($r = -0.34$, $p = 0.045$); but, other O_2 saturation variables did not show any relationships.

3.6. Regional putamen volume changes

Multiple regions within the putamen showed increased and decreased ratios of radial distance of surface points from the medial curve, indicating increased or decreased regional volume in OSA, compared to control subjects. Regions with decreased volumes within the putamen in OSA subjects included bilateral rostral (Fig. 2a, b, f, n, and q), mid-dorsal (Fig. 2c, g, and h), medial-caudal (Fig. 2d, j, and p), and mid-ventral sites (Fig. 2k, p), and increased volumes included the left caudal-dorsal (Fig. 2e), right mid-dorsal (Fig. 2i), left mid-ventral portions (Fig. 2l, m), and right caudal-ventral area (Fig. 2o).

3.7. Putamen volume and linear regression analyses

Regression analyses findings are summarized in Table 3. Oxygen saturation nadir ($p = 0.045$, $B = -20.46$) was an independent predictor for left global putamen volume in OSA subjects. However, no variable independently predicted right global putamen volume in these subjects.

4. Discussion

4.1. Overview

Newly-diagnosed, treatment-naïve OSA subjects show increased global putamen volumes, but localized areas within the putamen show both higher and lower volumes compared to control subjects. The appearance of both increased and decreased volumes suggests that we obtained a snapshot of progressive putamen tissue changes early in the development of the chronic OSA condition, in which both tissue swelling and loss occur, likely depending on the nature of the composite structure and local perfusion. The putamen sites with altered volume in OSA are associated with somatic and autonomic motor and neuropsychologic regulatory roles, all of which are deficient in the condition (Bedard et al., 1991; Beebe et al., 2003; Berry et al., 1986).

4.2. OSA and brain injury

The putamen, together with other basal ganglia and brain structures, shows gray matter volume loss, gray matter and fiber injury, and metabolic abnormalities in patients in chronic stages of the OSA syndrome (Kamba et al., 1997; Macey et al., 2002; Morrell et al., 2003), rather than the increased volume in the newly-diagnosed cases studied here. Those prior studies in chronic OSA subjects, based on volumetric procedures, showed reduced regional tissue volume changes, indicating chronic tissue injury with late OSA diagnosis (Macey et al., 2002; Morrell et al., 2003). However, in newly-diagnosed OSA subjects, acute tissue changes are predominantly accompanied by axonal, glial, and neuronal swelling, i.e., larger volumes, but show decreased mean diffusivity values in the same OSA subject pool, indicative of acute tissue injury (Kumar et al., 2012). The increased overall structural volumes found here should be viewed in this context of apparent injury from diffusion tensor imaging, but global increased volume from resultant swelling; the progression of the syndrome will be accompanied by later volume declines. The localized declines in volume may follow different time courses for different brain structures; selected brain areas, such as the mammillary bodies, show reduced volumes early in the disease process (Kumar et al., 2008). Moreover, subareas within the putamen may vary in vascularization and tissue composition with different time courses of tissue loss.

4.3. Global and regional putamen volumes and OSA functional changes

Global putamen volumes were significantly increased in OSA over control subjects, despite sub-regions showing both increased and decreased volumes. The putamen contains dopaminergic neurons, sends those projections to the substantia nigra and ventral tegmentum (Gorbachevskaya, 1997; Schultz and Romo, 1987), and receives projections from the thalamus, insular cortices, and prefrontal cortex (Avendano et al., 2006; Ferry et al., 2000), areas which are also injured in OSA subjects (Kumar et al., 2012; Macey et al., 2002, 2008). Putamen sub-regions are involved in various functions, including those heavily influenced by dopamine released by midbrain projections (Inase et al., 1997; Schultz, 1986).

Various putamen sites, including bilateral rostral, mid-dorsal, medial-caudal, mid-ventral and ventral, and caudal-dorsal regions showed either increased or decreased volume in OSA subjects; both types of tissue changes may be associated with altered function. The putamen primarily serves motor regulation functions, receiving projections from motor and somatosensory areas for that role (Kunzle, 1977). The rostral putamen receives projections from the prerubral area of the substantia nigra through the lateral hypothalamus, internal capsule and the head of the caudate nucleus (Usunoff et al., 1976). Somatosensory and motor cortex areas representing the lower limbs, ventromedial portions of facial regions, and upper limb regions project to the dorsolateral putamen, and these projecting sites send fibers in a

Table 2
Coefficients of correlation and significant values among putamen volumes, BMI, sleep, neuropsychologic variables, O_2 saturation, putamen MD values, and AHI in OSA subjects.

	Left putamen volume n = 43	Right putamen volume n = 43	BMI n = 43	ESS n = 43	PSQI n = 43	BDI-II n = 43	BAI n = 43	O2 saturation nadir n = 36	Left putamen MD n = 19	Right putamen MD n = 19	AHI n = 43
Left putamen volume		r = 0.980	r = −0.348	r = −0.212	r = −0.060	r = −0.213	r = −0.386	r = −0.336	r = −0.485	r = −0.440	r = −0.083
		p < 0.001	p = 0.022	p = 0.172	p = 0.700	p = 0.170	p = 0.011	p = 0.045	p = 0.035	p = 0.059	p = 0.597
Right putamen volume	r = 0.980		r = −0.320	r = −0.0194	r = −0.098	r = −0.209	r = −0.397	r = −0.307	r = −0.538	r = −0.461	r = −0.089
	p < 0.001		p = 0.036	p = 0.212	p = 0.532	p = 0.179	p = 0.008	p = 0.069	p = 0.017	p = 0.047	p = 0.569
BMI	r = −0.348	r = −0.320		r = 0.026	r = 0.039	r = −0.029	r = 0.090	r = 0.172	r = 0.315	r = 0.468	r = 0.433
	p = 0.022	p = 0.036		p = 0.867	p = 0.802	p = 0.854	p = 0.564	p = 0.317	p = 0.189	p = 0.043	p = 0.004
ESS	r = −0.212	r = −0.194	r = 0.026		r = 0.079	r = 0.241	r = 0.186	r = −0.034	r = 0.227	r = 0.283	r = 0.064
	p = 0.172	p = 0.212	p = 0.867		p = 0.615	p = 0.119	p = 0.232	p = 0.845	p = 0.350	p = 0.241	p = 0.682
PSQI	r = −0.060	r = −0.098	r = 0.039	r = 0.079		r = 0.611	r = 0.464	r = −0.121	r = 0.224	r = 0.036	r = 0.034
	p = 0.700	p = 0.532	p = 0.802	p = 0.615		p < 0.001	p = 0.002	p = 0.482	p = 0.356	p = 0.885	p = 0.827
BDI-II	r = −0.213	r = −0.209	r = 0.029	r = 0.241	r = 0.611		r = 0.806	r = 0.242	r = 0.517	r = 0.388	r = −0.010
	p = 0.170	p = 0.179	p = 0.854	p = 0.119	p < 0.001		p < 0.001	p = 0.156	p = 0.023	p = 0.101	p = 0.951
BAI	r = −0.386	r = −0.397	r = 0.090	r = 0.186	r = 0.464	r = 0.806		r = 0.390	r = 0.354	r = 0.243	r = −0.061
	p = 0.011	p = 0.008	p = 0.564	p = 0.232	p = 0.002	p < 0.001		p = 0.019	p = 0.138	p = 0.316	p = 0.699
O2 saturation nadir	r = −0.336	r = −0.307	r = 0.172	r = −0.034	r = −0.121	r = 0.242	r = 0.390		r = 0.072	r = 0.152	r = −0.206
	p = 0.045	p = 0.069	p = 0.317	p = 0.845	p = 0.482	p = 0.156	p = 0.019		p = 0.785	p = 0.560	p = 0.228
Left putamen MD	r = −0.485	r = −0.538	r = 0.315	r = 0.227	r = 0.224	r = 0.517	r = 0.354	r = 0.072		r = 0.817	r = 0.414
	p = 0.035	p = 0.017	p = 0.189	p = 0.350	p = 0.356	p = 0.023	p = 0.138	p = 0.785		p < 0.001	p = 0.078
Right putamen MD	r = −0.440	r = −0.461	r = 0.468	r = 0.283	r = 0.036	r = 0.388	r = 0.243	r = 0.152	r = 0.817		r = 0.425
	p = 0.059	p = 0.047	p = 0.043	p = 0.241	p = 0.885	p = 0.101	p = 0.316	p = 0.560	p < 0.001		p = 0.070
AHI	r = −0.083	r = −0.089	r = 0.433	r = 0.064	r = 0.034	r = −0.010	r = −0.061	r = −0.206	r = 0.414	r = 0.425	
	p = 0.597	p = 0.569	p = 0.004	p = 0.682	p = 0.827	p = 0.951	p = 0.699	p = 0.228	p = 0.078	p = 0.070	

BMI, body mass index; ESS, Epworth Sleepiness Scale; PSQI, Pittsburgh Sleep Quality Index; BDI-II, Beck Depression Inventory II; BAI, Beck Anxiety Inventory; MD, Mean diffusivity; AHI, apnea–hypopnea-index.

rostro-caudal direction (Kunzle, 1975, 1977). Both premotor and supplementary motor areas representing the face (Muakkassa and Strick, 1979), also send projections to the ventral medial putamen (Kunzle, 1978; Miyata and Sasaki, 1984). The ventrolateral globus pallidus projects to the ventrolateral thalamus, which represents oral and upper airway regions (DeVito and Anderson, 1982). Supplementary motor areas and the caudolateral substantia nigra are involved in orofacial control (Boussaoud and Joseph, 1985). Both the globus pallidus and substantia nigra sites receive projections from rostroventral putamen (DeVito et al., 1980). Since a principal concern in OSA is somatic motor regulation of the oral airway, localized damage to subareas of the putamen involved in such regulation is of great interest in the syndrome.

Multiple autonomic motor and neurobehavioral issues, including altered memory, attention, psychomotor and executive function, and emotional regulation are affected in OSA subjects (Bedard et al., 1991; Beebe et al., 2003; Berry et al., 1986). The putamen contains dopaminergic neurons, the neurotransmitter principally involved in mediating reward. Injury to ventral putamen sub-regions served by dopamine-based neurotransmitters would have significant effects on affective behaviors dependent on reward (Seeman et al., 2006); those behaviors are heavily affected in OSA (Asghari et al., 2012). A primary characteristic of OSA is impaired autonomic nervous system regulation, reflected especially in excessive sympathetic activity and impaired timing to autonomic challenges (Harper et al., 2003; Henderson et al., 2002; Somers et al., 1995). Injury to both the insular cortices and dorsal putamen likely contributes to that deficit, since both regions serve autonomic roles; the putamen receives projections from the insular cortices (Saper, 1982), and both structures show overall injury and functional deficits during autonomic and respiratory challenges (Henderson et al., 2004; Kumar et al., 2012; Macey et al., 2006). Since a close relationship exists between transient elevation in blood pressure with both diaphragmatic (Trelease et al., 1985) and upper airway action (Marks and Harper, 1987), and upper airway muscle suppression is more sensitive to blood pressure elevation than the diaphragm, distorted regulation of dynamic sympathetic patterns has the potential to contribute to the "motor neglect" of upper airway muscles found in OSA.

4.4. Tissue volume changes: processes

Several mechanisms may underlie the global and regional putamen tissue changes. OSA subjects are intermittently exposed to hypoxia from the repeated, successive cessations of airflow during sleep, which is followed by rapid re-oxygenation at apnea termination. Moreover, exaggerated blood pressure swings occur over the course of each apneic event, with substantial changes in perfusion accompanying the vascular alterations (Yan et al., 2009). Hypoxic and ischemic conditions induce energy pump failure, altering sodium and potassium ion distribution, and affecting intracellular and extracellular water, resulting in neuronal and axonal swelling (Hossmann, 1971; Lowry et al., 1964; Mintorovitch et al., 1994; Oehmichen et al., 2001). The axonal and neuronal swelling increases volumes of affected brain structures. However, chronic stages of hypoxia/ischemia would be accompanied by a reduction in axons, neurons, and glia, leaving a net loss of tissue volume over control values. Since OSA subjects showed higher global putamen volumes, relative to control subjects, we believe that the tissue changes are representative of acute changes. These changes likely contribute to manifestations of characteristics in OSA.

Both increased and decreased localized volume changes appeared in OSA subjects within the putamen over controls, suggesting that the changes result from both early and long-standing tissue alterations in these newly-diagnosed, treatment-naïve subjects, or that portions of the putamen may be more vulnerable to hypoxic or perfusion changes through the nature of tissue composition or extent of vascularization. Overall, the predominant changes appear to be in acute stages, since global putamen volumes were found to be significantly increased in OSA over controls. These findings suggest that a series of changes occurs

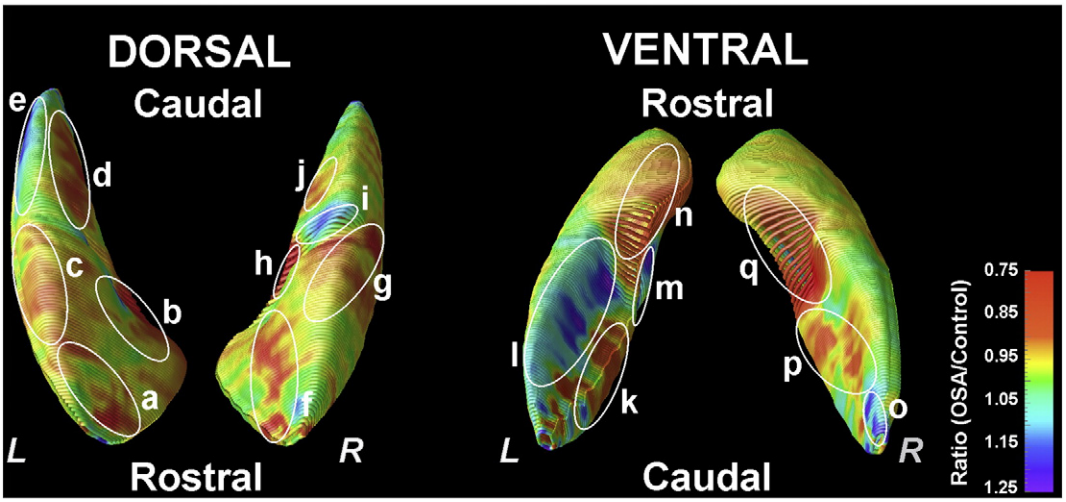

Fig. 2. Areas of regional putamen volume increase and decrease in OSA compared to control subjects, with areas shown from a dorsal perspective (Left), and a ventral perspective (Right). The color coding represents ratios of radial distance of each surface point from control reference values, with warm colors (*orange to red*) indicating volume losses and cool colors (*blue to purple*) representing volume increases; those corresponding sites are labeled with letters (a–q). Bilateral sites with increased putamen volume in the OSA group included mid and caudal-ventral portions, based on OSA to control group ratios, and decreased volumes emerged in bilateral rostral and mid-dorsal regions, extending to ventral areas (a–q).

within tissue before axonal and neuronal loss, with early, acute stages of pathology associated with increased tissue volume, while chronic stages of pathology are accompanied by decreased volumes. Tissue changes in both acute and chronic stages of pathology likely contribute to functional deficits served by subareas within the structure.

It is possible, although speculative, that the OSA condition may result from putamen tissue changes, i.e., that the failure in upper airway action results from initial putamen dysfunction from injury which may progress, cumulating with the exaggerated autonomic and other manifestations found in OSA. Initial putamen injury, perhaps by carbon monoxide poisoning, accidental hypoxic exposure, or reaction to toxic substances acting on the multiple neurotransmitters in the structure, has the potential to interfere with normal putamen functioning, disrupting normal regulation of the upper airway. This initial dysfunction may escalate to a condition that self-perpetuates or worsens, with all of the autonomic and somatomotor outcomes reported for OSA. Determination of the feasibility of such an outcome would require basic studies of insults to the putamen in an animal model that results in interference with upper airway muscle action paralleling the coordination loss found in human OSA.

Table 3
Comparison of multivariate p values and B values of AHI, BMI, sleep, neuropsychologic, left and right putamen MD values, and O_2 saturation variables for the linear regression analyses in OSA subjects.

Side	Covariates	Multivariate p values	B
Left putamen volume	AHI	0.573	–
	BMI	0.175	–
	ESS	0.892	–
	PSQI	0.950	–
	BDI–II	0.897	–
	BAI	0.567	–
	O_2 saturation nadir	0.045	–20.46
Right putamen volume	AHI	–	–
	BMI	–	–
	ESS	–	–
	PSQI	–	–
	BDI-II	–	–
	BAI	–	–
	O_2 saturation nadir	–	–

AHI, apnea–hypopnea-index; BMI, body mass index; ESS, Epworth Sleepiness Scale; PSQI, Pittsburgh Sleep Quality Index; BDI-II, Beck Depression Inventory II; BAI, Beck Anxiety Inventory; MD, mean diffusivity.

4.5. Limitations

One limitation of this study is the absence of data on the pre-diagnosis duration of OSA subjects. However, we are reasonably confident that the predominant brain tissue changes in the OSA subjects are acute in nature. MRI-based mean diffusivity (MD) procedures, which measure water diffusion within tissue, and are influenced by the presence of tissue barriers and extracellular/extra-axonal fluid, show reduced MD values in acute disease stages of ischemic/hypoxic pathology, but show increased values in chronic stages of such pathology (Ahlhelm et al., 2002; Chan et al., 2009; Hossmann et al., 1994; Loubinoux et al., 1997; Matsumoto et al., 1995; Shereen et al., 2011; Warach et al., 1996). Since these same OSA subjects showed reduced MD values across various brain sites (Kumar et al., 2012), we believe that the predominant tissue pathology in this sample derives from damage in acute stages.

5. Conclusions

Newly-diagnosed OSA subjects without treatment show significantly increased global putamen volumes over control subjects, with subregions within the structure showing both increased and decreased volumes. Regional sites with decreased volumes emerged in rostral, mid-dorsal, medial-caudal, and mid-ventral areas, and increased volumes appeared in caudal-dorsal, mid-dorsal, mid-ventral, and caudal-ventral portions. These areas contribute to regulation of neuropsychologic, autonomic motor, and somatomotor functions deficient in OSA, and especially to oral motor functioning, a special concern in the syndrome due to airway collapse in obstructive apnea. The pathological processes contributing to tissue changes may include intermittent hypoxia and impaired perfusion, both of which can affect glial tissue necessary for neuronal support; such tissue is extremely sensitive to hypoxia and ischemia. The finding of regional increased and decreased volume variation indicates that final volume loss earlier found in long-term OSA occurs with a progression of changes in the tissue.

Acknowledgments

The authors thank Ms. Rebecca Harper, Mr. Edwin Valladares, and Drs. Rebecca Cross and Stacy Serber for their help with data collection, and Mr. Jose Palomares for his help in table preparation. This research

work was supported by the National Institutes of Health R01 HL-113251.

References

1999. Sleep-related breathing disorders in adults: recommendations for syndrome definition and measurement techniques in clinical research. The Report of an American Academy of Sleep Medicine Task Force. Sleep 22, 667–689.

Ahlhelm, F., Schneider, G., Backens, M., Reith, W., Hagen, T., 2002. Time course of the apparent diffusion coefficient after cerebral infarction. Eur. Radiol. 12, 2322–2329.

Alexander, G.E., Crutcher, M.D., 1990. Preparation for movement: neural representations of intended direction in three motor areas of the monkey. J. Neurophysiol. 64, 133–150.

Alkan, A., Sharifov, R., Akkoyunlu, M.E., Kilicarslan, R., Toprak, H., Aralasmak, A., Kart, L., 2013. MR spectroscopy features of brain in patients with mild and severe obstructive sleep apnea syndrome. Clin. Imaging 37, 989–992.

Asghari, A., Mohammadi, F., Kamrava, S.K., Tavakoli, S., Farhadi, M., 2012. Severity of depression and anxiety in obstructive sleep apnea syndrome. Eur. Arch. Otorhinolaryngol. 269, 2549–2553.

Avendano, C., de Las Heras, S., Gimenez-Amaya, J.M., 2006. Striatal projections from the lateral and posterior thalamic complexes. An anterograde tracer study in the cat. Histochem. Cell Biol. 125, 265–271.

Badgaiyan, R.D., Fischman, A.J., Alpert, N.M., 2008. Explicit motor memory activates the striatal dopamine system. Neuroreport 19, 409–412.

Beck, A.T., Epstein, N., Brown, G., Steer, R.A., 1988. An inventory for measuring clinical anxiety: psychometric properties. J. Consult. Clin. Psychol. 56, 893–897.

Beck, A.T., Steer, R.A., Brown, G.K., 1996. Manual for the Beck Depression Inventory-II. The Psychological Corporation, San Antonio, Texas.

Bedard, M.A., Montplaisir, J., Richer, F., Rouleau, I., Malo, J., 1991. Obstructive sleep apnea syndrome: pathogenesis of neuropsychological deficits. J. Clin. Exp. Neuropsychol. 13, 950–964.

Beebe, D.W., Groesz, L., Wells, C., Nichols, A., McGee, K., 2003. The neuropsychological effects of obstructive sleep apnea: a meta-analysis of norm-referenced and case-controlled data. Sleep 26, 298–307.

Berry, D.T., Webb, W.B., Block, A.J., Bauer, R.M., Switzer, D.A., 1986. Nocturnal hypoxia and neuropsychological variables. J. Clin. Exp. Neuropsychol. 8, 229–238.

Booth, J.R., Wood, L., Lu, D., Houk, J.C., Bitan, T., 2007. The role of the basal ganglia and cerebellum in language processing. Brain Res. 1133, 136–144.

Boussaoud, D., Joseph, J.P., 1985. Role of the cat substantia nigra pars reticulata in eye and head movements. II. Effects of local pharmacological injections. Exp. Brain Res. 57, 297–304.

Bowman, E.M., Aigner, T.G., Richmond, B.J., 1996. Neural signals in the monkey ventral striatum related to motivation for juice and cocaine rewards. J. Neurophysiol. 75, 1061–1073.

Butters, M.A., Aizenstein, H.J., Hayashi, K.M., Meltzer, C.C., Seaman, J., Reynolds 3rd, C.F., Toga, A.W., Thompson, P.M., Becker, J.T., 2009. Three-dimensional surface mapping of the caudate nucleus in late-life depression. Am. J. Geriatr. Psychiatry 17, 4–12.

Chan, K.C., Khong, P.L., Lau, H.F., Cheung, P.T., Wu, E.X., 2009. Late measures of microstructural alterations in severe neonatal hypoxic-ischemic encephalopathy by MR diffusion tensor imaging. Int. J. Dev. Neurosci. 27, 607–615.

Cross, R.L., Kumar, R., Macey, P.M., Doering, L.V., Alger, J.R., Yan-Go, F.L., Harper, R.M., 2008. Neural alterations and depressive symptoms in obstructive sleep apnea patients. Sleep 31, 1103–1109.

DeVito, J.L., Anderson, M.E., 1982. An autoradiographic study of efferent connections of the globus pallidus in Macaca mulatta. Exp. Brain Res. 46, 107–117.

DeVito, J.L., Anderson, M.E., Walsh, K.E., 1980. A horseradish peroxidase study of afferent connections of the globus pallidus in Macaca mulatta. Exp. Brain Res. 38, 65–73.

Emin Akkoyunlu, M., Kart, L., Kilicarslan, R., Bayram, M., Aralasmak, A., Sharifov, R., Alkan, A., 2013. Brain diffusion changes in obstructive sleep apnoea syndrome. Respiration 86, 414–420.

Ferry, A.T., Ongur, D., An, X., Price, J.L., 2000. Prefrontal cortical projections to the striatum in macaque monkeys: evidence for an organization related to prefrontal networks. J. Comp. Neurol. 425, 447–470.

Gorbachevskaya, A.I., 1997. Projections of the ventral tegmental area of the midbrain, the substantia nigra, and the amygdaloid body in different parts of the putamen in the dog. Neurosci. Behav. Physiol. 27, 496–502.

Harper, R.M., Macey, P.M., Henderson, L.A., Woo, M.A., Macey, K.E., Frysinger, R.C., Alger, J.R., Nguyen, K.P., Yan-Go, F.L., 2003. fMRI responses to cold pressor challenges in control and obstructive sleep apnea subjects. J. Appl. Physiol. 94, 1583–1595.

Henderson, L.A., Macey, P.M., Macey, K.E., Frysinger, R.C., Woo, M.A., Harper, R.K., Alger, J.R., Yan-Go, F.L., Harper, R.M., 2002. Brain responses associated with the Valsalva maneuver revealed by functional magnetic resonance imaging. J. Neurophysiol. 88, 3477–3486.

Henderson, L.A., Richard, C.A., Macey, P.M., Runquist, M.L., Yu, P.L., Galons, J.P., Harper, R.M., 2004. Functional magnetic resonance signal changes in neural structures to baroreceptor reflex activation. J. Appl. Physiol. 96, 693–703.

Hossmann, K.A., 1971. Cortical steady potential, impedance and excitability changes during and after total ischemia of cat brain. Exp. Neurol. 32, 163–175.

Hossmann, K.A., Fischer, M., Bockhorst, K., Hoehn-Berlage, M., 1994. NMR imaging of the apparent diffusion coefficient (ADC) for the evaluation of metabolic suppression and recovery after prolonged cerebral ischemia. J. Cereb. Blood Flow Metab. 14, 723–731.

Husain, M.M., McDonald, W.M., Doraiswamy, P.M., Figiel, G.S., Na, C., Escalona, P.R., Boyko, O.B., Nemeroff, C.B., Krishnan, K.R., 1991. A magnetic resonance imaging study of putamen nuclei in major depression. Psychiatry Res. 40, 95–99.

Iber, C., Ancoli-Israel, S., Chesson, A., Quan, S.F., 2007. for the American Academy of Sleep Medicine, The AASM Manual for the Scoring of Sleep and Associated Events: Rules, Terminology and Technical Specifications1st ed. American Academy of Sleep Medicine, Westchester, Illinois.

Inase, M., Li, B.M., Tanji, J., 1997. Dopaminergic modulation of neuronal activity in the monkey putamen through D1 and D2 receptors during a delayed Go/Nogo task. Exp. Brain Res. 117, 207–218.

Johns, M.W., 1991. A new method for measuring daytime sleepiness: the Epworth sleepiness scale. Sleep 14, 540–545.

Kamba, M., Suto, Y., Ohta, Y., Inoue, Y., Matsuda, E., 1997. Cerebral metabolism in sleep apnea. Evaluation by magnetic resonance spectroscopy. Am. J. Respir. Crit. Care Med. 156, 296–298.

Knutson, K.L., Rathouz, P.J., Yan, L.L., Liu, K., Lauderdale, D.S., 2006. Stability of the Pittsburgh Sleep Quality Index and the Epworth Sleepiness Questionnaires over 1 year in early middle-aged adults: the CARDIA study. Sleep 29, 1503–1506.

Kumar, R., Birrer, B.V., Macey, P.M., Woo, M.A., Gupta, R.K., Yan-Go, F.L., Harper, R.M., 2008. Reduced mammillary body volume in patients with obstructive sleep apnea. Neurosci. Lett. 438, 330–334.

Kumar, R., Ahdout, R., Macey, P.M., Woo, M.A., Avedissian, C., Thompson, P.M., Harper, R.M., 2009a. Reduced caudate nuclei volumes in patients with congenital central hypoventilation syndrome. Neuroscience 163, 1373–1379.

Kumar, R., Macey, P.M., Cross, R.L., Woo, M.A., Yan-Go, F.L., Harper, R.M., 2009b. Neural alterations associated with anxiety symptoms in obstructive sleep apnea syndrome. Depress. Anxiety 26, 480–491.

Kumar, R., Nguyen, H.D., Ogren, J.A., Macey, P.M., Thompson, P.M., Fonarow, G.C., Hamilton, M.A., Harper, R.M., Woo, M.A., 2011. Global and regional putamen volume loss in patients with heart failure. Eur. J. Heart Fail. 13, 651–655.

Kumar, R., Chavez, A.S., Macey, P.M., Woo, M.A., Yan-Go, F.L., Harper, R.M., 2012. Altered global and regional brain mean diffusivity in patients with obstructive sleep apnea. J. Neurosci. Res. 90, 2043–2052.

Kunzle, H., 1975. Bilateral projections from precentral motor cortex to the putamen and other parts of the basal ganglia. An autoradiographic study in Macaca fascicularis. Brain Res. 88, 195–209.

Kunzle, H., 1977. Projections from the primary somatosensory cortex to basal ganglia and thalamus in the monkey. Exp. Brain Res. 30, 481–492.

Kunzle, H., 1978. An autoradiographic analysis of the efferent connections from premotor and adjacent prefrontal regions (areas 6 and 9) in macaca fascicularis. Brain Behav. Evol. 15, 185–234.

Loubinoux, I., Volk, A., Borredon, J., Guirimand, S., Tiffon, B., Seylaz, J., Meric, P., 1997. Spreading of vasogenic edema and cytotoxic edema assessed by quantitative diffusion and T2 magnetic resonance imaging. Stroke 28, 419–426 (discussion 426–417).

Lowry, O.H., Passonneau, J.V., Hasselberger, F.X., Schulz, D.W., 1964. Effect of ischemia on known substrates and cofactors of the glycolytic pathway in brain. J. Biol. Chem. 239, 18–30.

Macey, P.M., Henderson, L.A., Macey, K.E., Alger, J.R., Frysinger, R.C., Woo, M.A., Harper, R.K., Yan-Go, F.L., Harper, R.M., 2002. Brain morphology associated with obstructive sleep apnea. Am. J. Respir. Crit. Care Med. 166, 1382–1387.

Macey, K.E., Macey, P.M., Woo, M.A., Henderson, L.A., Frysinger, R.C., Harper, R.K., Alger, J.R., Yan-Go, F., Harper, R.M., 2006. Inspiratory loading elicits aberrant fMRI signal changes in obstructive sleep apnea. Respir. Physiol. Neurobiol. 151, 44–60.

Macey, P.M., Kumar, R., Woo, M.A., Valladares, E.M., Yan-Go, F.L., Harper, R.M., 2008. Brain structural changes in obstructive sleep apnea. Sleep 31, 967–977.

Macey, P.M., Woo, M.A., Kumar, R., Cross, R.L., Harper, R.M., 2010. Relationship between obstructive sleep apnea severity and sleep, depression and anxiety symptoms in newly-diagnosed patients. PLoS One 5, e10211.

Macey, P.M., Kumar, R., Yan-Go, F.L., Woo, M.A., Harper, R.M., 2012. Sex differences in white matter alterations accompanying obstructive sleep apnea. Sleep 35, 1603–1613.

Macey, P.M., Kumar, R., Woo, M.A., Yan-Go, F.L., Harper, R.M., 2013. Heart rate responses to autonomic challenges in obstructive sleep apnea. PLoS One 8, e76631.

Marks, J.D., Harper, R.M., 1987. Differential inhibition of the diaphragm and posterior cricoarytenoid muscles induced by transient hypertension across sleep states in intact cats. Exp. Neurol. 95, 730–742.

Matsumoto, K., Lo, E.H., Pierce, A.R., Wei, H., Garrido, L., Kowall, N.W., 1995. Role of vasogenic edema and tissue cavitation in ischemic evolution on diffusion-weighted imaging: comparison with multiparameter MR and immunohistochemistry. Am. J. Neuroradiol. 16, 1107–1115.

Mintorovitch, J., Yang, G.Y., Shimizu, H., Kucharczyk, J., Chan, P.H., Weinstein, P.R., 1994. Diffusion-weighted magnetic resonance imaging of acute focal cerebral ischemia: comparison of signal intensity with changes in brain water and Na+, K(+)-ATPase activity. J. Cereb. Blood Flow Metab. 14, 332–336.

Miyata, M., Sasaki, K., 1984. Horseradish peroxidase studies on thalamic and striatal connections of the mesial part of area 6 in the monkey. Neurosci. Lett. 49, 127–133.

Morrell, M.J., McRobbie, D.W., Quest, R.A., Cummin, A.R., Ghiassi, R., Corfield, D.R., 2003. Changes in brain morphology associated with obstructive sleep apnea. Sleep Med. 4, 451–454.

Muakkassa, K.F., Strick, P.L., 1979. Frontal lobe inputs to primate motor cortex: evidence for four somatotopically organized 'premotor' areas. Brain Res. 177, 176–182.

Oehmichen, M., Ochs, U., Meissner, C., 2001. Regional potassium distribution in the brain in forensic relevant types of intoxication preliminary morphometric evaluation using a histochemical method. Neurotoxicology 22, 99–107.

Pastakia, B., Polinsky, R., Di Chiro, G., Simmons, J.T., Brown, R., Wener, L., 1986. Multiple system atrophy (Shy-Drager syndrome): MR imaging. Radiology 159, 499–502.

Sabattoli, F., Boccardi, M., Galluzzi, S., Treves, A., Thompson, P.M., Frisoni, G.B., 2008. Hippocampal shape differences in dementia with Lewy bodies. Neuroimaging 41, 699–705.

Saper, C.B., 1982. Convergence of autonomic and limbic connections in the insular cortex of the rat. J. Comp. Neurol. 210, 163–173.
Sapir, A., Kaplan, J.B., He, B.J., Corbetta, M., 2007. Anatomical correlates of directional hypokinesia in patients with hemispatial neglect. J. Neurosci. 27, 4045–4051.
Schultz, W., 1986. Responses of midbrain dopamine neurons to behavioral trigger stimuli in the monkey. J. Neurophysiol. 56, 1439–1461.
Schultz, W., Romo, R., 1987. Responses of nigrostriatal dopamine neurons to high-intensity somatosensory stimulation in the anesthetized monkey. J. Neurophysiol. 57, 201–217.
Seeman, P., Wilson, A., Gmeiner, P., Kapur, S., 2006. Dopamine D2 and D3 receptors in human putamen, caudate nucleus, and globus pallidus. Synapse 60, 205–211.
Shereen, A., Nemkul, N., Yang, D., Adhami, F., Dunn, R.S., Hazen, M.L., Nakafuku, M., Ning, G., Lindquist, D.M., Kuan, C.Y., 2011. Ex vivo diffusion tensor imaging and neuropathological correlation in a murine model of hypoxia–ischemia-induced thrombotic stroke. J. Cereb. Blood Flow Metab. 31, 1155–1169.
Shi, J., Wang, Y., Ceschin, R., An, X., Lao, Y., Vanderbilt, D., Nelson, M.D., Thompson, P.M., Panigrahy, A., Lepore, N., 2013. A multivariate surface-based analysis of the putamen in premature newborns: regional differences within the ventral striatum. PLoS One 8, e66736.
Somers, V.K., Dyken, M.E., Clary, M.P., Abboud, F.M., 1995. Sympathetic neural mechanisms in obstructive sleep apnea. J. Clin. Invest. 96, 1897–1904.
Thompson, P.M., Hayashi, K.M., De Zubicaray, G.I., Janke, A.L., Rose, S.E., Semple, J., Hong, M.S., Herman, D.H., Gravano, D., Doddrell, D.M., Toga, A.W., 2004. Mapping hippocampal and ventricular change in Alzheimer disease. Neuroimaging 22, 1754–1766.
Trelease, R.B., Sieck, G.C., Marks, J.D., Harper, R.M., 1985. Respiratory inhibition induced by transient hypertension during sleep in unrestrained cats. Exp. Neurol. 90, 173–186.
Usunoff, K.G., Hassler, R., Romansky, K., Usunova, P., Wagner, A., 1976. The nigrostriatal projection in the cat. Part 1. Silver impregnation study. J. Neurol. Sci. 28, 265–288.
Wallace, A., Bucks, R.S., 2013. Memory and obstructive sleep apnea: a meta-analysis. Sleep 36, 203–220.
Warach, S., Mosley, M., Sorensen, A.G., Koroshetz, W., 1996. Time course of diffusion imaging abnormalities in human stroke. Stroke 27, 1254–1256.
Yan, B., Li, L., Harden, S.W., Gozal, D., Lin, Y., Wead, W.B., Wurster, R.D., Cheng, Z.J., 2009. Chronic intermittent hypoxia impairs heart rate responses to AMPA and NMDA and induces loss of glutamate receptor neurons in nucleus ambiguous of F344 rats. Am. J. Physiol. Regul. Integr. Comp. Physiol. 296, R299–R308.